High NA Microscope Objective with Depth-Dependent Spherical Aberration Correction

Cory Kaspar[1*], Ethan Luker [1*], Linden Solgonick [1*], Matias Straub Martinez [1*]
[1]Wyant College of Optical Sciences, University of Arizona, Tucson, AZ 85719

ABSTRACT

Microsoft's Project Silica is developing a long-term and sustainable storage method by storing data in fused silica plates. This allows for safe data storage that will not require continuous updates onto new storage media as technology develops. We are designing a microscope objective to be used to read and write data on these glass plates. Our project aims to design a microscope objective capable of writing data voxels into fused silica plates, with plans to extend the design's scope to reading voxels in the future. The objective has a high numerical aperture (NA) to resolve signals from specific voxels within the glass. It is also capable of focusing at various depths within the glass, as data is stored throughout the medium. Additionally, it utilizes index-matching immersion oil between the objective and silica designed to control spherical aberration, which becomes more prevalent with a higher NA and at greater optical depths within the silica.

1. LAB REQUIREMENTS

1.1 Introduction

This project aims to design a high NA microscope objective for use in Microsoft's Project Silica data storage initiative. Within one optical system, the objective aims to serve both as a femtosecond laser write and widefield illumination read objective. At a minimum, our objective must achieve a NA of 0.6 at a primary write wavelength of 516 nm, producing an acceptable diffraction-limited focal spot within the fused silica or borosilicate glass substrates. The substrates will be up to 2 mm thick, so discrete voxel layers must be accurately created to this depth. The dominant optical challenge lies in depth-dependent spherical aberration (SA), which increases continuously as the focal plane of the objective translates from the bottom to the top layer of the substrate. Index matching immersion oil between the front element of the objective and the substrate will substantially reduce the air-glass interface SA, but residual depth-dependent SA will increase as the focal plane translates deeper into the glass, driven by index differences between the oil and the substrate. The lens design of the objective must therefore consider this aberration and correct the variation of SA. Ideally, we will use commercially available optics, COTS optics, to reduce the cost of manufacturing. The current procedure for reading symbols images them directly through broadband LED transmission microscopy, so the objective will need to correct both axial and lateral chromatic aberration to produce acceptable images for symbol decoding.

1.2 Technical Requirements

Optical systems designed for three-dimensional data storage in silica must maintain high-resolution focus while operating at various depths in the material. The customer requires an optical objective capable of both writing and reading data embedded in Silica. The system must maintain a high spatial resolution at varying depths, requiring a NA of at least 0.6 to resolve signal of adjacent voxels. This helps achieve a tight focus on data inscription. A greater NA would increase writing efficiency and decrease voxel volume but introduce more significant spherical aberration as depth increases. A key requirement is the correction of spherical aberration introduced by refractive index mismatch between air and silica. We should also correct spherical aberration using commercially available optics, COTS optics, to reduce the cost of manufacturing. Additionally, the system's Strehl intensity ratio (SIR) shall be greater than 0.8, to ensure diffraction-limited performance.

* Further author information:
Cory Kaspar: kaspar@arizona.edu
Ethan Luker: ethanluker@arizona.edu
Linden Solgonick: lindensolgonick@arizona.edu
Matias Straub Martinez: mstraubmartinez@arizona.edu

Table 1: Required Technical Specifications

Parameter	Specification
Numerical Aperture	≥ 0.6
Wavelength	516 nm
Objective Magnification	40X
Working Distance	2 mm
Beam Diameter	5 mm
HFOV	0.1°
Strehl Intensity Ratio	> 0.8
Focus depth	0 to 2 mm

2. FIRST ORDER DESIGN

We developed a common first order design to meet system specifications, primarily focusing on the writing function of the objective. The incoming light is defined as a 5 mm beam having a very narrow bandwidth centered on 516 nm, approximately a single wavelength. Each system must account for writing at various depths in the fused silica plate, up to 2 mm deep. Our initial design uses classical lens design theory to develop a system that meets the requirements. This design incorporates a classic lister objective, initially designed for 10x magnification. The lister objective is composed of two achromatic doublets using NBK7 and NSF6 Schott glasses to correct for early chromatic aberration with use of a broadband light source, such as for reading applications of the objective. The lister lens is approximately aplanatic and followed by a duo of cascaded aplanatic elements to increase the numerical aperture of the system. Finally, there is a layer of immersion oil between the final aplanatic element and the fused silica plate, the thickness of which is adjusted for focusing at various depths using the zoom feature in Code V. The lens layouts for focusing at the surface (position 1), 1 mm below the surface (position 2), and at the 2 mm extent of the fused silica plate (position 3) are shown below from left to right. This is a thin lens design, with finite lens thickness applied to show the shape of each lens more clearly.

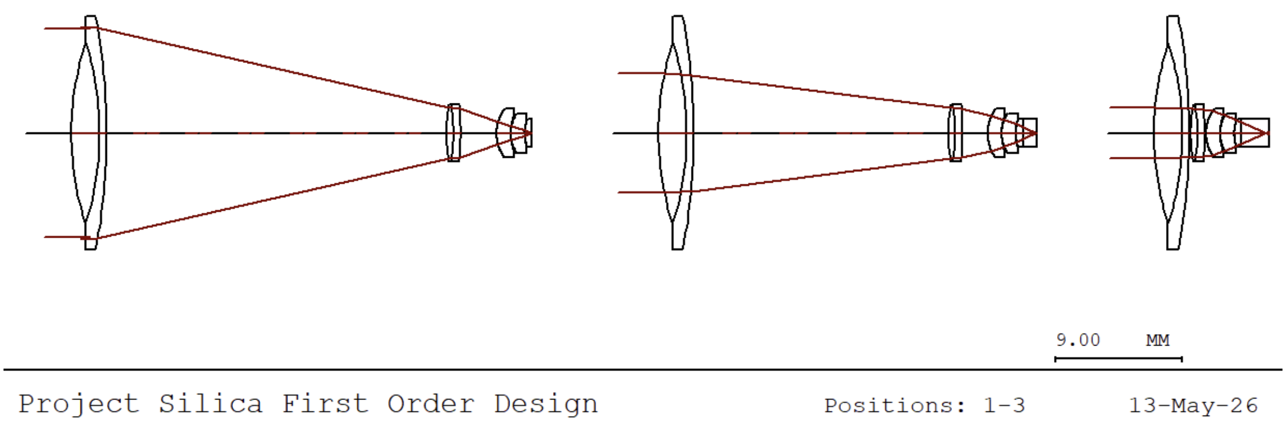

Figure 1: First Order Design Lens Layouts

This approach required iterative alterations to improve the first order design and address spherical aberration in the third order design. Notably, our initial first order design changed the thickness of the immersion oil to adjust the focusing depth, while later designs change the gap between the two doublets in the lister objective to keep the immersion oil at a realistic thickness of 0.5 mm. The space between the two lens elements was altered for each zoom position. To address spherical aberration in our third order designs, we also implemented a low power air spaced doublet preceding the optical system shown above. These issues are addressable without major alterations to the first order design, and as such we considered this design to be promising in its approximate alignment with technical specifications and potential for optimization.

3. THIRD ORDER DESIGNS

3.1 Cory's 3rd Order Design

A brief analysis of the aberrations in the system indicates the only significant aberrations are field curvature and spherical aberration, with all other Seidel aberrations being entirely corrected. Since the field of view of the system is small, field curvature is negligible, so spherical aberration dominates. Chromatic aberration would theoretically also be highly problematic, but this system is modeled for a single wavelength laser beam to optimize for the objective's writing function. Several corrections were employed for chromatic aberration by optimizing for spherical aberration, as well as the two achromatic doublets in the lister lens, which makes the design adjustable for reading voxels without significant alteration. To account for dependence on the depth of the beam focus within the fused silica plate, both the air spacing in the initial doublet and the distance between the doublet and the main objective system. Third order optimization of the system yields significantly decreased aberration compared to the first order and third order unoptimized systems, such that the RMS spot size for each focusing depth is on the order of tenths of a micron. The associated lens layouts and spot diagrams for each system are shown below.

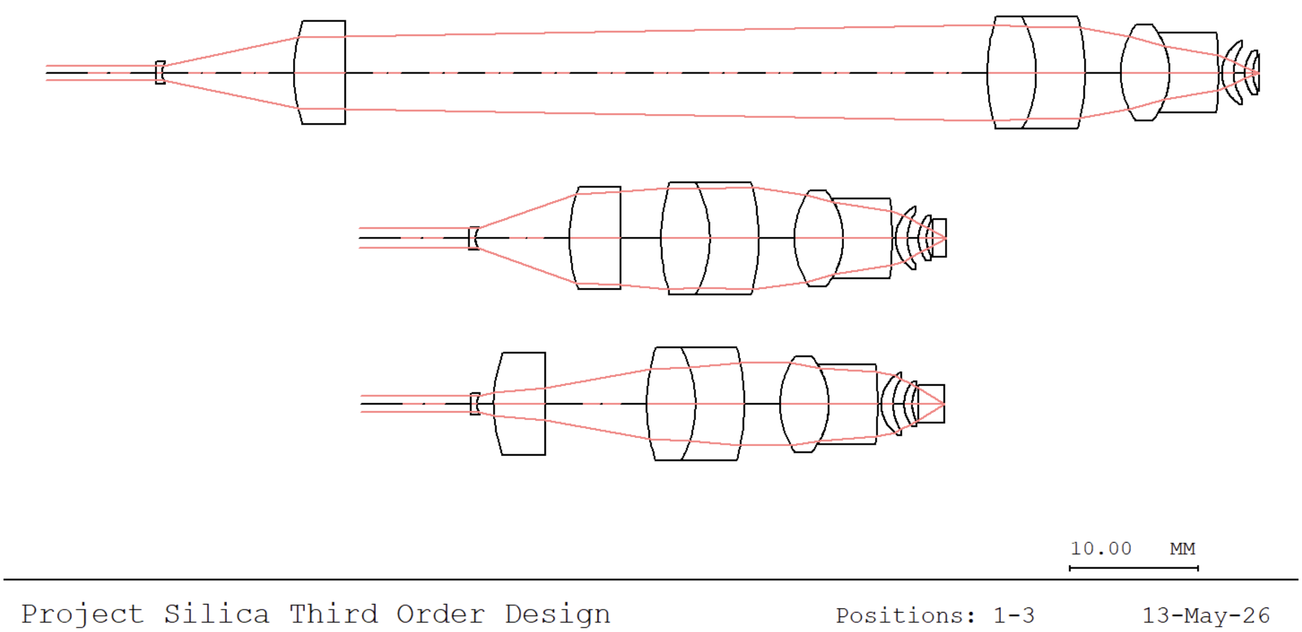

Figure 2: Cory's Third Order design lens layouts, showing all zoom positions.

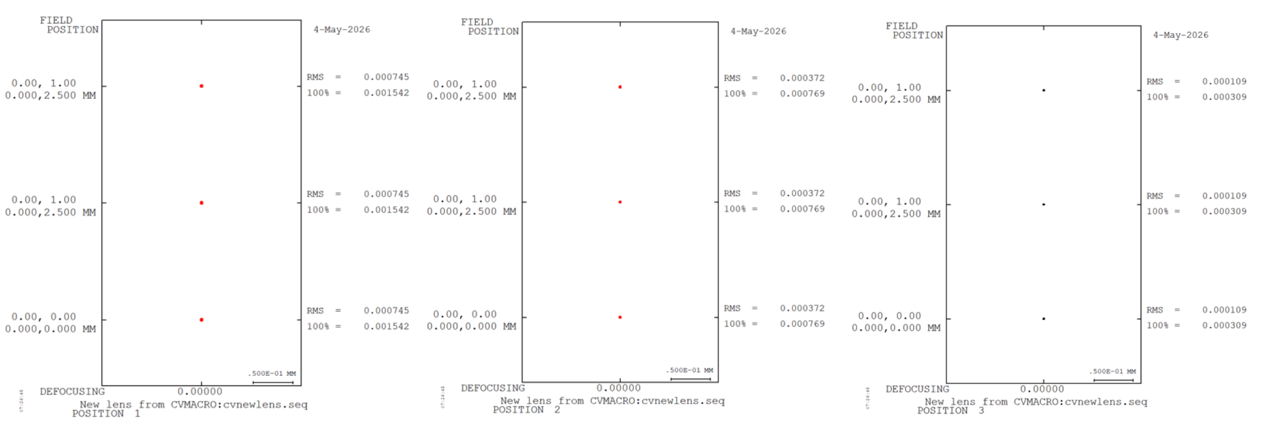

Figure 3: Cory's Third Order design spot diagrams, showing Positions 1-3 from left to right.

3.2 Ethan's 3rd Order Design

This design focuses on using a lister objective. There are two variables to adjust zoom in the system, first being the distance between an air spaced zero power achromatic doublet and second being the separation between the two doublets in the system. Along with the two achromatic doublets, there are also two aplanatic elements. With the current optimization, SA is completely minimized for all three zoom points, and the largest spot size is around 0.72 um and the lowest Strehl ratio is 0.906.

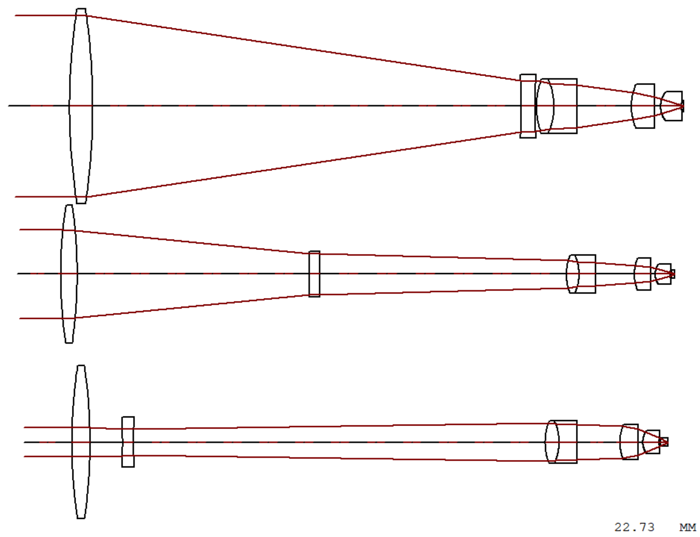

Figure 4: Ethan's Third Order design lens layout and spot diagram for zoom position 3 (2 mm into silica plate).

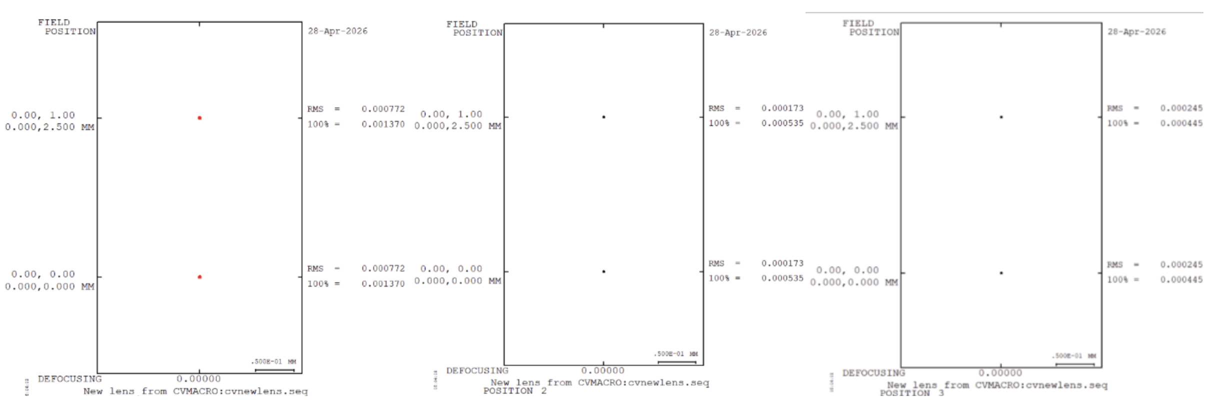

Figure 5: Ethan's Third Order design spot diagrams, showing Positions 1-3 from left to right.

3.3 Linden's 3rd Order Design

This design consists of an aspheric lens followed by two achromatic doublets and three singlets. The final singlet is flush with index matching immersion oil. The thickness of the immersion oil is fixed at 0.5mm for all three zoom positions, as a thick layer of immersion oil would be unrealistic. The aspheric lens helps to correct for the spherical aberration. The focus between the three zoom positions was adjusted by changing the spacing between the two achromatic doublets. All three zoom positions achieved an NA 0.606 and near diffraction limited spot diagrams with minimal aberrations. The primary aberrations are spherical aberration and field curvature. Spherical aberration is minimized, and field curvature is negligible due to the low field of view. Additionally, this design utilizes one COTS element, Edmund Optics COTS 12.5mm #47-690, as the second achromatic lens. The design is optimized to write at a 516nm wavelength as used in Project Silica, and therefore chromatic aberration would need to be further addressed in future designs, as the two doublets do not fully correct for axial chromatic aberration. The primary drawback of this design is the large system length in zoom position 3.

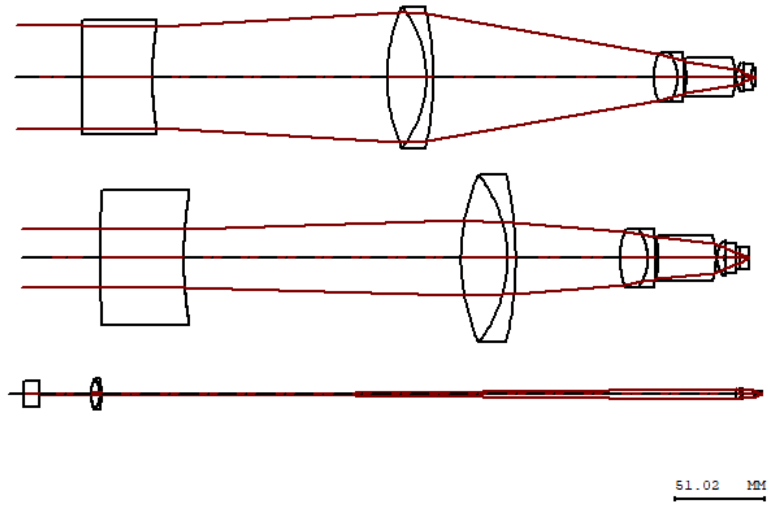

Figure 6: Linden's Third Order design lens layouts, showing all zoom positions.

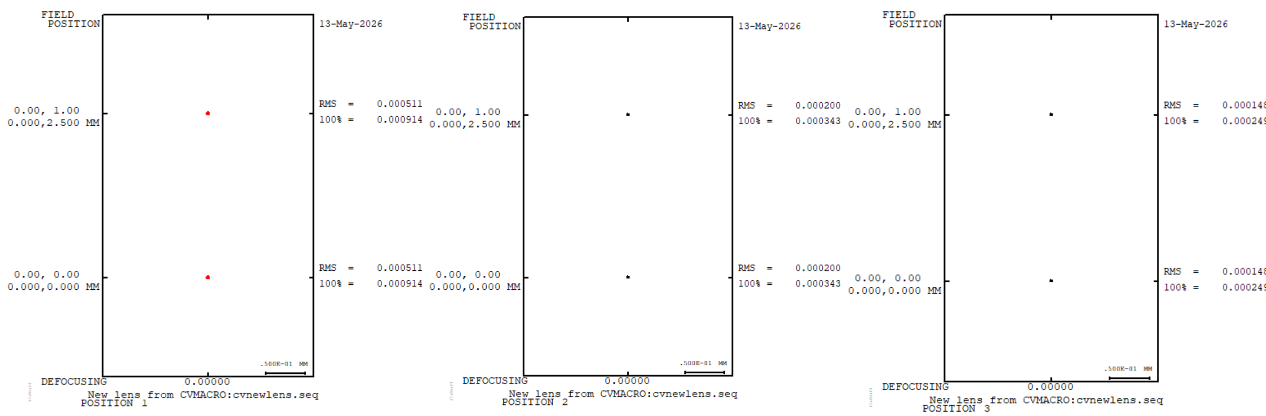

Figure 7: Linden's Third Order design spot diagrams, showing Positions 1-3 from left to right.

3.4 Matias' 3rd Order Design

This design is optimized for a single-wavelength architecture at a wavelength of 516 nm for writing into fused silica. An afocal corrector pair provides spherical aberration compensation across 0 to 2 mm silica depth. The objective comprises two positive singlets followed by an aplanatic meniscus corrector pair. Zoom functionality is distributed between the afocal corrector spacing and the spacing between the singlets. Oil immersion defines the entrance medium, and no commercial optics were used in favor of custom optimization for minimal spot size at the write focal plane.

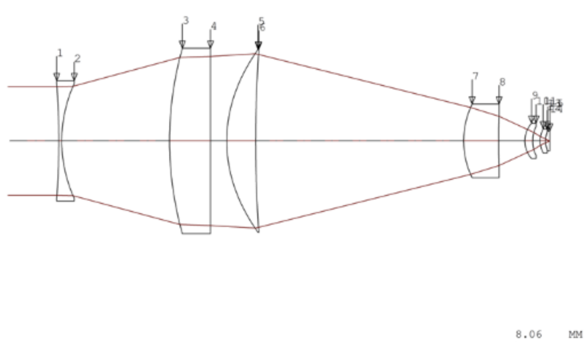

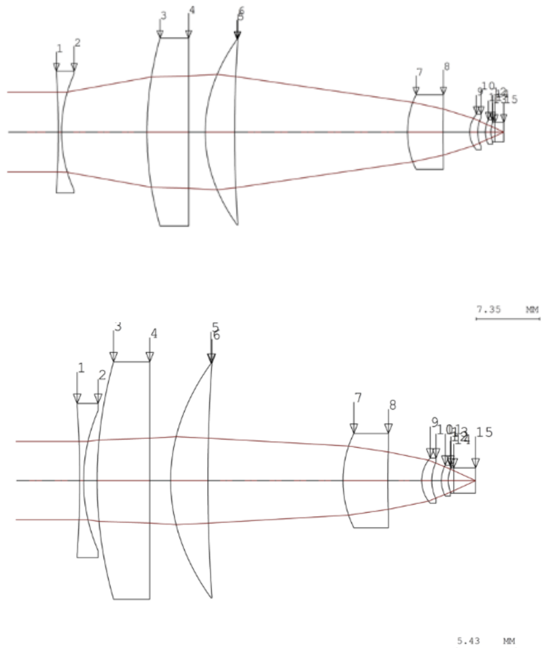

Figure 8: Matias' Third Order design lens layouts, showing all zoom positions.

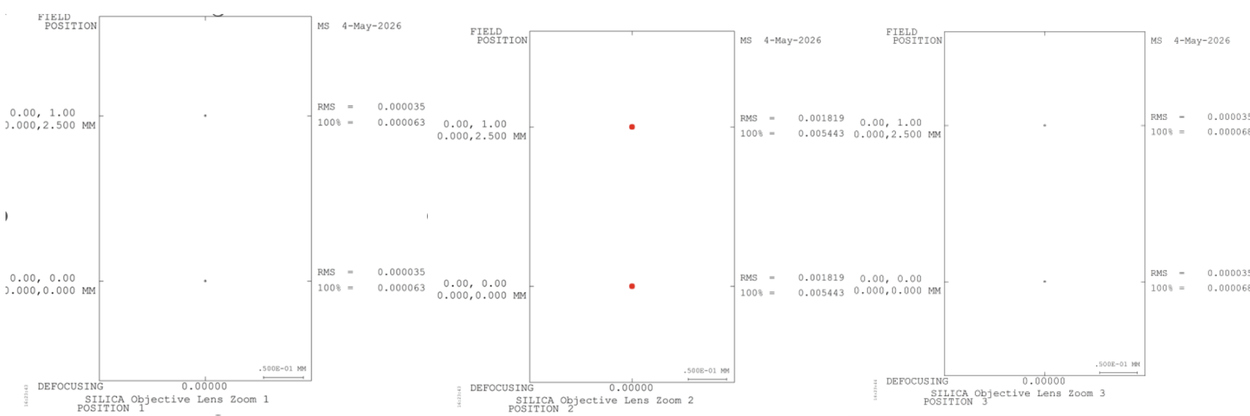

Figure 9: Matias' Third Order design spot diagrams, showing Positions 1-3 from left to right.

4. FINAL OPTIMIZATION AND TOLERANCE ANALYSIS

4.1 Cory's Optimization and Tolerancing

This design aims to demonstrate potential performance of the system using custom components, achieving high performance both as designed and as built. The design has a NA of 0.6, with an RMS spot size under a micron for all writing depths. The effective focal length of each zoom position is around 1.5 mm, and the overall length varies between 85.92 mm for focusing at the top of the plate down to 35.88 mm when focusing at the extent of the plate. The RMS differential tolerancing and point spread function are shown below for each of the three focusing positions. The requirement of SIR is met, > 0.8 in every case, achieving a minimum SIR of 0.963 at the surface of the fused silica plate and improving with writing depth. This design achieves a monochromatic RMS wavefront error < 0.1 at over 90% probability for all the fields and 3 writing depths. In tolerancing, compensators were added or working distance and spherical aberration, specifically variance in thickness between and directly following the low power air spaced doublet, thickness of the immersion oil, and decenter at the first aplanatic element. The tolerances for many of the parameters, especially the aplanatic elements, are somewhat tight, such that the system mechanical design will have to be carefully assembled.

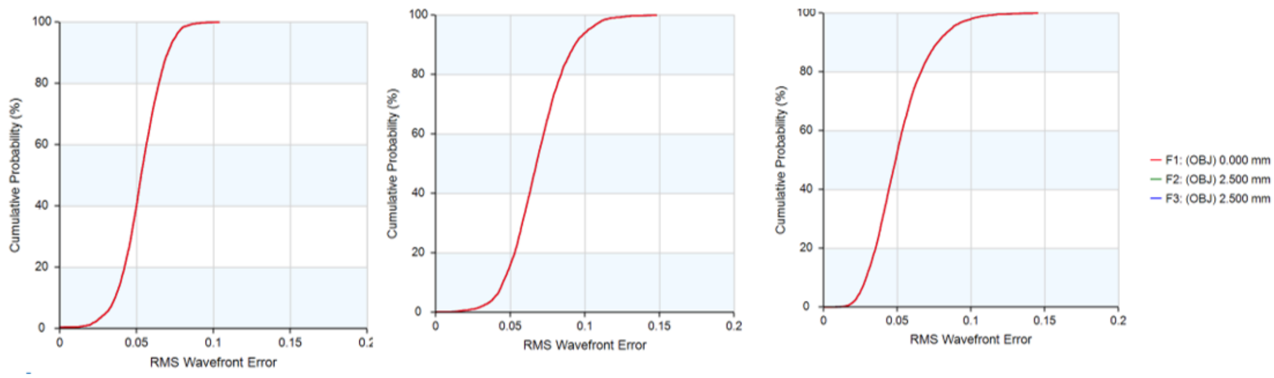

Figure 10: Cory's PSF plots for Strehl Ratio, showing Positions 1-3 from left to right

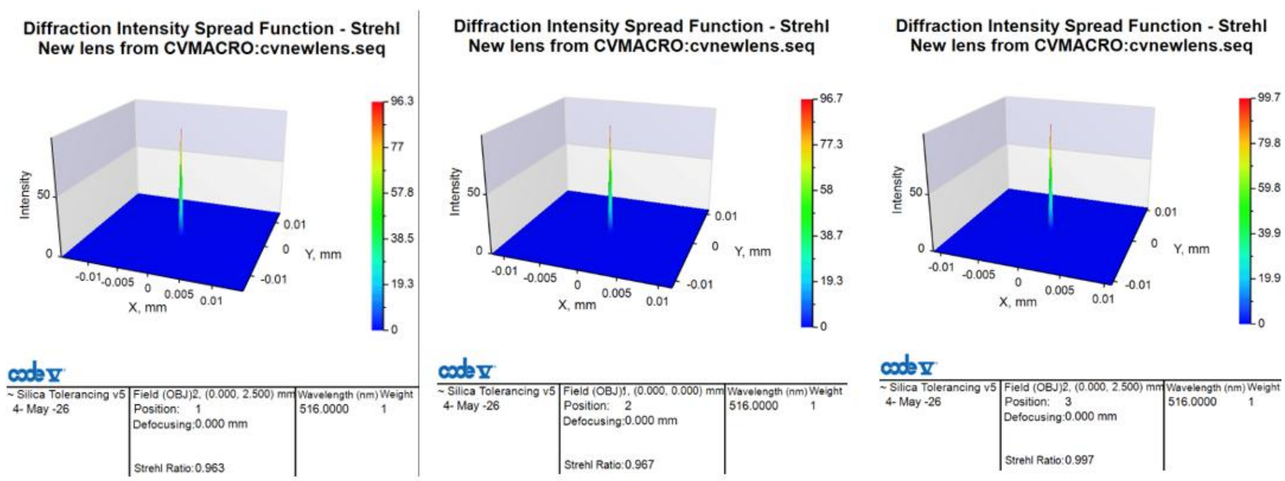

Figure 11: Cory's PSF plots for Strehl Ratio, showing Positions 1-3 from left to right.

4.2 Ethan's Optimization and Tolerancing

This design is very similar to the initial third order design with the only major change being one of the zoom parameters. The two zoom points in this system are the distance between the air spaced zero power achromatic doublet and the separation between the second doublet and the first aplanatic element. Spherical aberration is completely minimized for all three zoom points, the largest spot size is around 0.56 um, and the lowest Strehl ratio is 0.939 (Zoom 2, shown below). The main system improvements from the last iteration were a shortening of the whole system while maintaining the NA of 0.6 and further improving spot size and Strehl ratio. This was primarily done with changing one of the zooming parameters. When tolerancing, the most critical tolerances were the thickness, primarily the separation between the doublets, thickness of immersion oil, and the 2nd aplanatic element. Looking lens by lens the most problematic lens when it came to tolerancing was the second aplanatic element. This was due to it doing the most lens bending out of all the lenses.

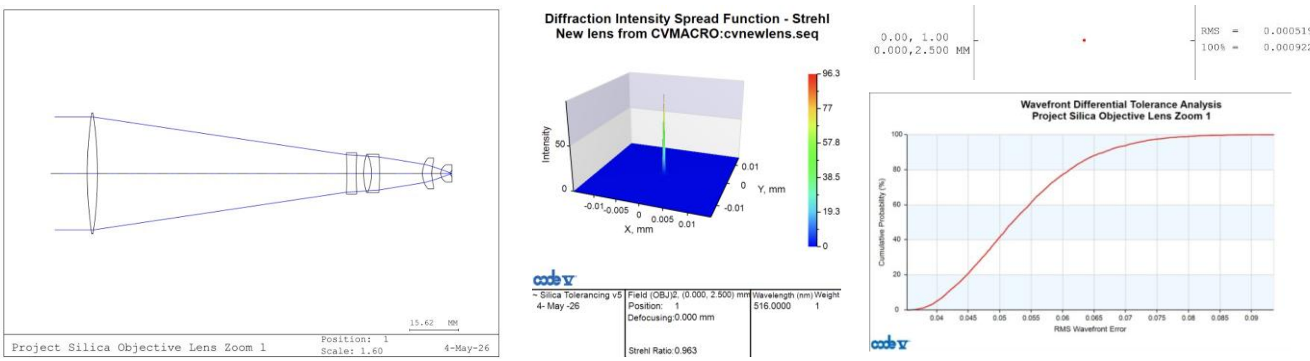

Figure 12: Ethan's Final Third Order design lens layout and spot diagram for zoom position 1 (0 mm into silica plate).

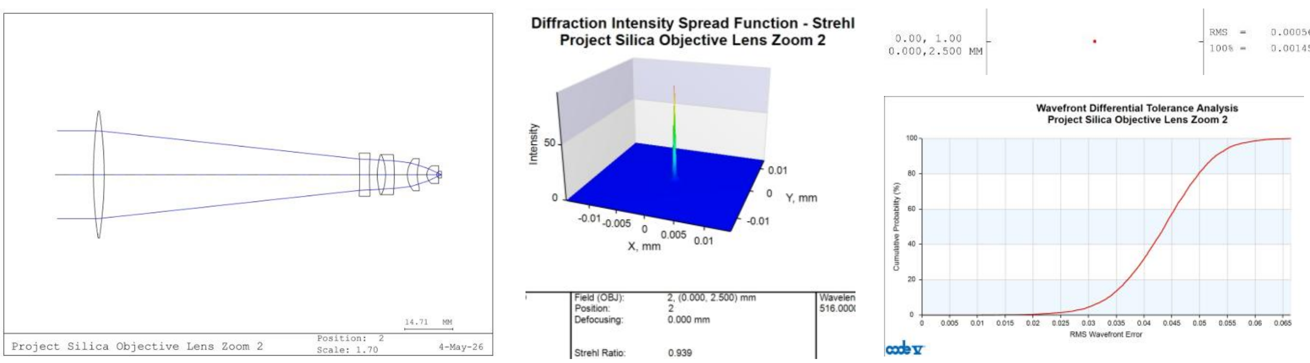

Figure 13: Ethan's Final Third Order design lens layout and spot diagram for zoom position 2 (1 mm into silica plate).

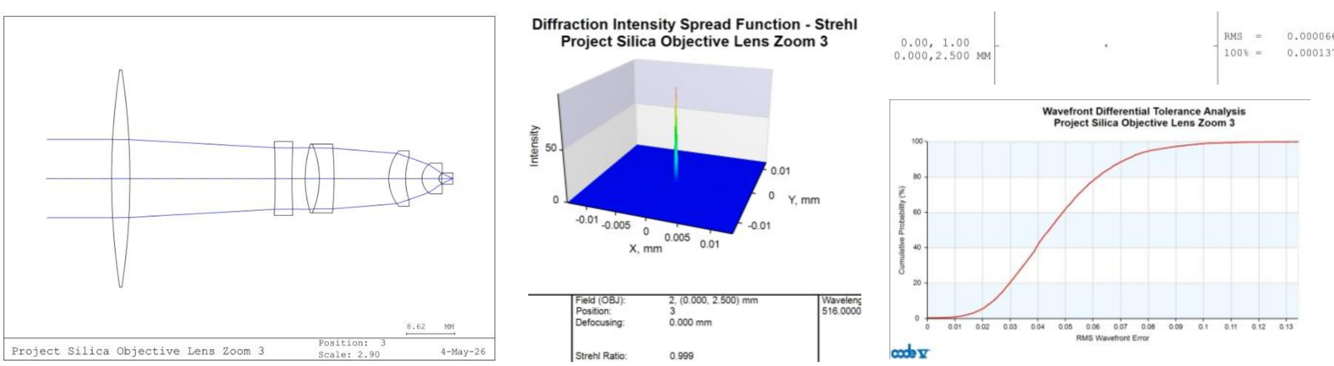

Figure 14: Ethan's Final Third Order design lens layout and spot diagram for zoom position 3 (2 mm into silica plate).

4.3 Linden's Optimization and Tolerancing

This design matched the original third order design, with the only change being slight optimization changes varying radii of curvature of the final three elements and spacings between the two achromatic doublets to account for commercial immersion oil and fused silica medium, Thorlab's immersion oil MOIL-30 and Corning's fused silica HPFS7980. All three zoom positions achieved a high Strehl intensity ratio, with the lowest being only 0.905 (see figure XXX) at focus of 0mm within the silica. After tolerancing, all three zoom positions achieved an RMS wavefront error of under 0.128 for 90% of trials. Tolerances for wavefront error were the poorest for focus 2mm within the silica. Zoom positions focusing at 0mm at 1mm depths achieved a near 100% probability of below 0.1 wavefront error, while zoom at 2mm depth only achieved a 90% probability below 0.128 wavefront error. Compensators were added for thickness of surface 12, power of surface 13, cylinder fringe irregularity at 0° for surface 1, and cylinder fringe irregularity at 45° for surface 6. Note that the tolerances for many parameters, especially for the final three elements, are tight, so the system's construction would need to be precise.

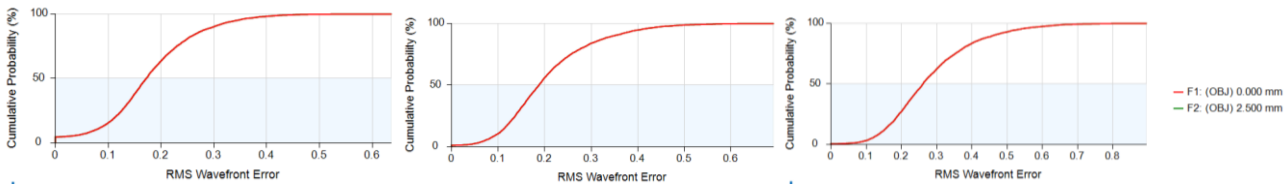

Figure 15: Linden's RMS Tolerance Analysis Plots, showing Positions 1-3 from left to right

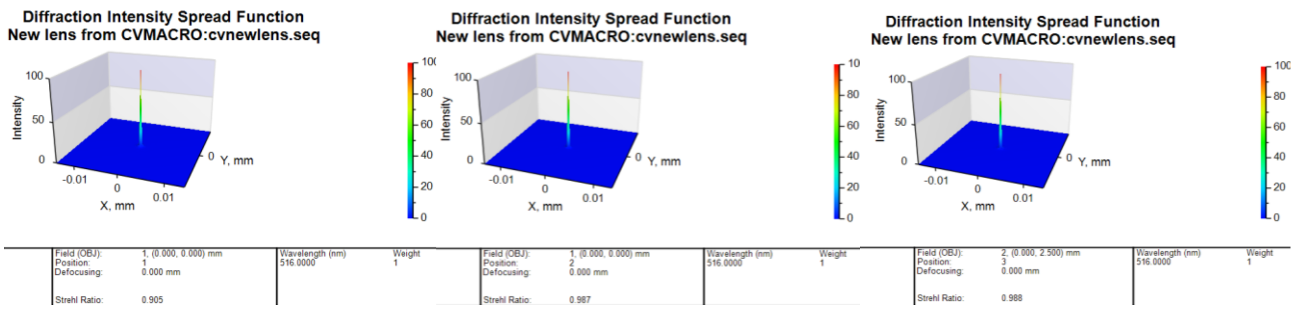

Figure 16: Linden's PSF plots for Strehl Ratio, showing Positions 1-3 from left to right.

4.4 Matias' Optimization and Tolerancing

Optical performance across the zoom range varies with depth compensation. At Positions 1 and 3 (0mm and 2mm silica), the design achieves diffraction-limited performance with Strehl Intensity ratios of 1.0 and negligible RMS wavefront error. At position 2, the performance degrades to Strehl 0.8 with RMS wavefront error ~0.1 waves at the 95th percentile. Wavefront differential tolerance analysis helped identify four critical compensators. These included thickness variation on surfaces 4 and 13, surface irregularity on surface 1 (at 0° azimuth), and combined irregularity and fringe on S3 (45° azimuth). The third-order optical layout remains unchanged, only tolerance values were added. In general, the system exhibits higher sensitivity to manufacturing tolerances, requiring tighter specification to these compensators by a factor of five to ten of the default CodeV values.

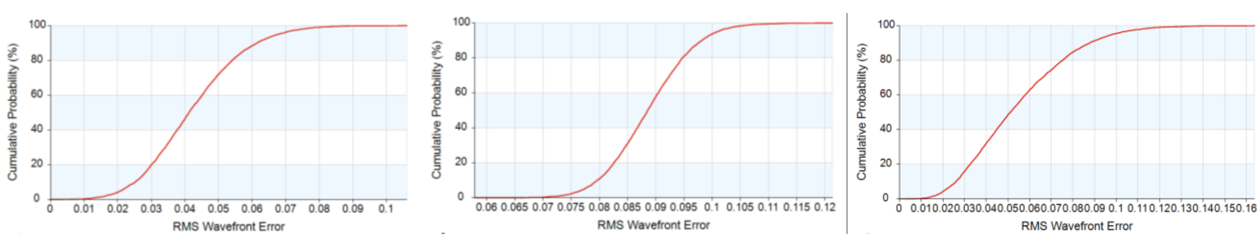

Figure 17: Matias' RMS Tolerance Analysis Plots, showing Positions 1-3 from left to right

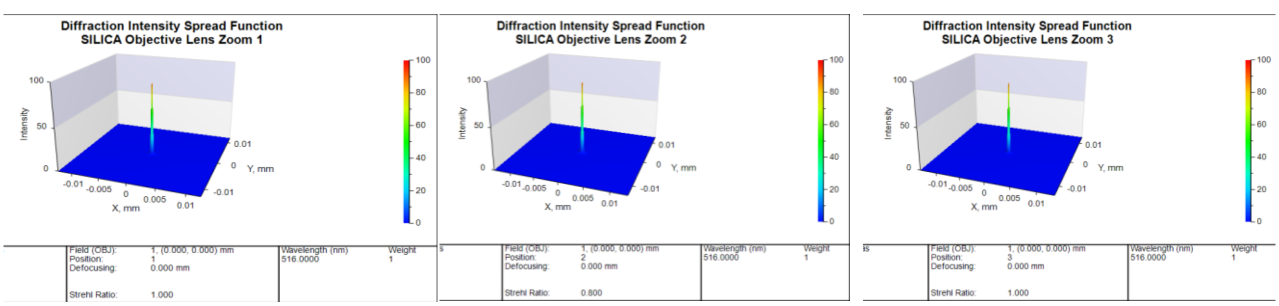

Figure 18: Matias' PSF Plots for Strehl Ratio, showing Positions 1-3 from left to right

5. CONCLUSION AND COMPARISON OF DESIGNS

	Requirement	Cory	Ethan	Linden	Matias
Numerical Aperture	≥ 0.6	0.6 / 0.6 / 0.6	0.6 / 0.6 / 0.6	0.606 / 0.606 / 0.606	0.6 / 0.6 / 0.6
Working Distance [mm]	0.5 / 1.5 / 2.5	0.502 / 1.498 / 2.500	0.5 / 1.5 / 2.5	0.5 / 1.5 / 2/5	0.500 / 1.500 / 2.500
RMS spot size [um]	< 2 microns	0.745 / 0.392 / 0.109	0.519 / 0.566 / 0.066	0.511 / 0.200 / 0.148	0.350 / 1.8 / 0.350
Strehl Ratio	> 0.8	0.963 / 0.967 / 0.997	9.52 / 9.39 / 9.99	0.905 / 0.987 / 0.988	1 / 0.8 / 1
RMS Wavefront Error at 90% probability	≤ 0.1	0.069 / 0.093 / 0.082	0.065 / 0.055 / 0.075	0.064 / 0.07 / 0.125	0.07 / 0.1 / 0.09

Table 2. Comparison of requirements for all designs

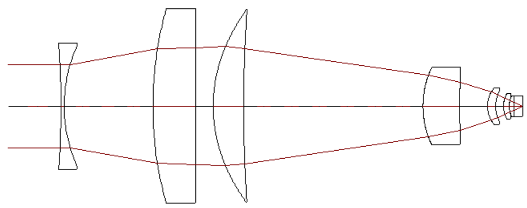

Figure 19: Matias' Final Design Layout (Position 2)

All team members were successful in creating a functional microscope objective that met the primary project requirements and demonstrated good imaging performance within the given constraints. Future improvements could include implementing more commercially available off-the-shelf (COTS) components to make the system more affordable. Adjusting our design to be suitable for reading voxels as well as writing them would require optimizing the systems for broadband illumination with multiple wavelengths and improving chromatic aberration correction across the visible spectrum. Among the designs, Matias's Design appeared to be the most promising because it had the shortest overall system length, successfully met the required project goals and objectives, and demonstrated the most even tolerancing behavior across the zoom positions. All systems required precise tolerancing to maintain image quality and performance, although future redesigns could reduce sensitivity to alignment and fabrication errors. The aplanatic elements significantly bent rays, which caused them to require tighter tolerancing than the other elements in the systems.

ACKNOWLEDGEMENTS

We would like to thank Dr. Yuzuru Takashima for his guidance throughout this project, and all those at Microsoft who have worked towards sustainable data storage through Project Silica.

REFERENCES

[1] Y. Zhang and H. Gross, "Systematic Design of Microscopic Lenses," Optical Design and Fabrication 2017 (Freeform, IODC, OFT), OSA Technical Digest (online) (Optica Publishing Group, 2017), paper IW4A.1.

[2] E. Gibney, "Microsoft team creates 'revolutionary' data-storage system that lasts for millennia," vol. 650, Nature, no. 8103 (2026): 807–808; https://doi.org/10.1038/d41586-026-00502-2.

[3] Microsoft Research Project Silica Team, "Laser writing in glass for dense, fast and efficient archival data storage," vol. 650, *Nature*, 606–612 (2026); https://doi.org/10.1038/s41586-025-10042-w.

[4] Y. Takashima, "Lecture slides," University of Arizona (2026).

[5] Microsoft Research, "Project Silica," Microsoft Research Project Page (2026); https://www.microsoft.com/en-us/research/project/project-silica/.